ORIGINAL PAPER

Mesoscale simulation on patterned nanotube model for amphiphilic block copolymer

Shou-Hong Yang · Yuen-Kit Cheng · Shi-Ling Yuan

Abstract Self-assembly of AB diblock copolymer confined in concentric-cylindrical nanopores was studied using MesoDyn simulation. Our calculation shows that in this confined geometry a zoo of exotic structures can be formed. These structures include bicontinuous phases like carbon nanotube, imperfect single helixes and double helixes. Moreover, the dependence of the chain conformation on the volume fraction, concentration, the interactions between blocks and the diameter of the cylindrical pore are investigated. The results of these simulations can be used to predict the diblock copolymer morphologies confined in concentric-cylindrical nanopores and should be helpful in designing polymeric nanomaterials in the future.

Keywords Block copolymer · Mesoscale simulation · Patterned model

Introduction

In recent years, a surge of research interests has been directed to the synthesis and properties of nanotubes for their various applications. Nanotubes have been made from a variety of materials including carbon, ceramics, metals or polymers [1–3]. Recent syntheses were concentrated on the self-assembly or template techniques. A case in point, carbon, polypeptide and polyaniline nanotubes have been prepared by self-assembly [4–7]; whereas conductive, poly (p-xylylene) and Nylon fibers have been made via templating [8, 9]. Macromolecular self-assembly has been revealed as an efficient and effective means in creating structures at nano-scale. Specifically, the confinement effects of boundaries influence self-assembly processes and lead to novel mesostructures. The self-assembly morphologies of block copolymers have found many applications in soft nanotechnology, drug delivery and even served as templates for fabricating advanced materials [10]. For self-assembled aggregates, the patterned nanostructures play a critical role in the applications. In order to facilitate a better understanding of the pattern formation besides experimental efforts, computer simulation is a promising in silico tool in offering efficient evaluation of aggregate formation and properties of nanotubes [11–13].

In principle, quantum or molecular mechanical methodologies would furnish detailed electronic and atomic information for the investigation of nanotubes, they are highly infeasible to be adopted in studying the properties of nanotubes at the nanoscale level of a reasonably representative-sized model needed to be used. Therefore, coarse-graining or mesoscopic simulations must be resorted to for the study of nanotube or nanotube template at the mesoscale level. Recently, Monte Carlo simulations [14, 15] based on coarse-graining models and mesoscopic simulations based on MesoDyn [16] or dissipative particle dynamics [17] have been able to identify transitions between stacked disks and curved lamellar in symmetric diblock copolymer melts confined in nanotubes. The single helix found in experiments has also been reproduced by simulations [18, 19]. And some more complex morphologies such as double helixes, triple helixes, lamellar parallel

S.-H. Yang · S.-L. Yuan (✉)
Key Lab of Colloid and Interface Chemistry,
Shandong University,
Jinan 250100, China
e-mail: shilingyuan@sdu.edu.cn

Y.-K. Cheng (✉)
Department of Chemistry, Hong Kong Baptist University,
Hong Kong, China
e-mail: ykcheng@hkbu.edu.hk

to the axis, mesh structures have been identified by simulations and calculations in diblock copolymer melts confined in nanotubes [20–22]. These simulations have provided useful insights about the self-assembly aggregates in the confined nanotube on the mesoscale level.

In this paper, we investigate nanotube template formation from amphiphilic **AB** block copolymer using mesoscale simulation based on MesoDyn method [23–30]. This method can reduce degrees of freedom for a large system size and obtain the properties of nanotubes in less time than the simulations on other lengths, especially the first report in the confined model [25] using this method gave us more confined idea. The effects of the block volume fraction, the polymer concentration, the interaction of block and solvent, and the pore diameter on the morphology transitions of symmetric and asymmetric cases are examined in details.

Model and calculations

The basic idea of MesoDyn simulation is that the Helmholtz free energy F of an inhomogeneous liquid is a function of the local density function ρ, from which all thermodynamic functions can be derived. The MesoDyn model consists of various types of beads with intramolecular interactions approximated by harmonic oscillator potentials. In this way, monomer densities are preserved without taking into account polymer chain dynamics and hydrodynamic interactions. Compared with the conventional particle simulation methods, field-based methods like MesoDyn have relatively high computational efficiency enabling significant advances in the investigation of microphase separation of block amphiphilic copolymers [31–33]. In these simulations, different patterned nanotubes with several tens of nanometer are modeled.

Each nanotube model of various radii was first placed in the center of a simulation box. To avoid artifacts resulting from applying periodic boundary conditions, ample space

has been made between the nanotube surface and the boundaries of the computational box. In the simulation, the polymer concentration outside the nanotube model was set to zero. Different patterned structures were generated by quenching a homogeneous solution of polymer surfactant. Certain amounts of solvent molecules were released locally or globally following the quench, depending on the particular morphology being formed. The patterned nanotube was analyzed as an isosurface of solvent or block copolymer in a self-consistent-field condition finally. Simulation was terminated whenever the order parameters converged to a set tolerance. The order parameter is indicative of the dynamics of phase separation. It represents the mean-squared deviation from homogeneity in the system and captures the effects of both phase separation and compressibility [34–36].

The chemical nature of the system in the MesoDyn method is defined by two sets of parameters: one is the chain topology in terms of the repeating segments (or beads), and the other is the interaction between the various components. For the first set, the MesoDyn method uses a Gaussian chain "spring-and-beads" description [37–40], in which all segments are of the same size, and the chain topology depends on the coarsened degrees of freedom of the original system. In our simulation, we focused on the Pluronics solution. Pluronics are block copolymers of poly (ethylene oxide) (PEO) and poly(propylene oxide) (PPO). In the chain topology of Pluronics, each bead or statistical unit corresponds to 4.3 ethylene oxide (EO) monomers (as one solvophilic solvent bead A) and 3.3 propylene oxide (PO) monomers (as one solvophobic solvent bead B) [41–44]. Secondly, the interaction energies of the various types of segments represent the pairwise interactions of beads. It is based on the regular solution theory and similar to the Flory-Huggins model. The interaction parameters can be considered in the context of non-ideal interaction. It is characterized by $\varepsilon_{AB} > 0$ as the repulsion between two components. Here, the diblock polymeric surfactant A_nB_{N-n}

Fig. 1 Morphologies of A_nB_{N-n} polymer surfactant nanotubes. Solvent-phase concentration field (scale on the right) for different block ratios $f = n/N$, $N=20$. (**a**) 0.25, (**b**) 0.30, (**c**) 0.40, (**d**) 0.50
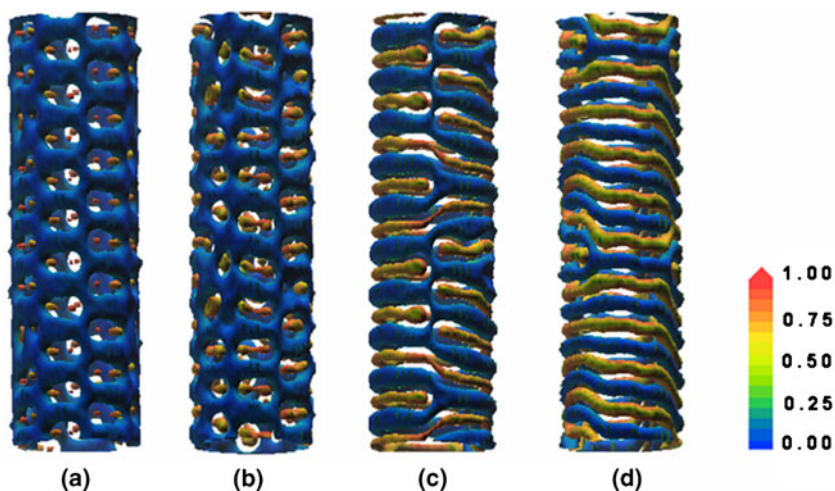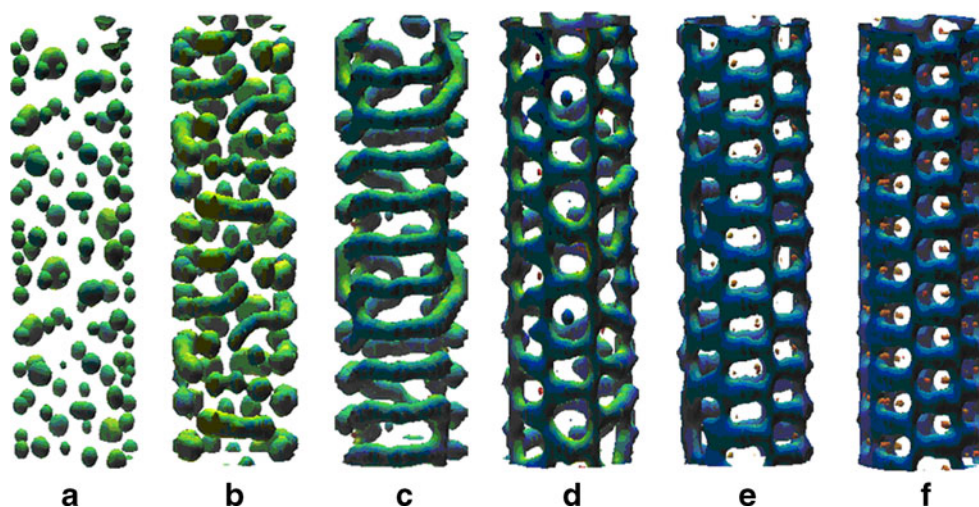
Fig. 2 Concentration of polymer in the solution, f=0.25 and N=20. (**a**) 25 vol%, (**b**) 35 vol%, (**c**) 45 vol%, (**d**) 55 vol%, (**e**) 65 vol%, (**f**) 75 vol%. Solvent-phase concentration field is as shown in Fig. 1

are parameterized by $\chi_{AB} \bullet N = 60$, $\chi_{AS}/\chi_{AB} = 0.47$ and $\chi_{AS}/\chi_{BS} = 0.82$ (*i.e.*, when N=20, χ_{AB}=3.0). These parameters are similar to the ones in the Fraaije's work[29, 30, 32, 34, 40]. They represent the binary interaction strengths among components A (slightly solvophilic), B (slightly solvophobic), and S (solvent, like water). In the mean-field model any polymer surfactant solution with the same property the scaled interaction parameters will behave in exactly the same way. The parameters defined here were compared with the experimental microphase diagrams of concentrated Pluronic aqueous solution [10]. With the selected parameters, χ_{ij}, N and n, the polymers are all made insoluble in the nanotube. Hence, the deformations of the nanotubes are at constant mass of polymer.
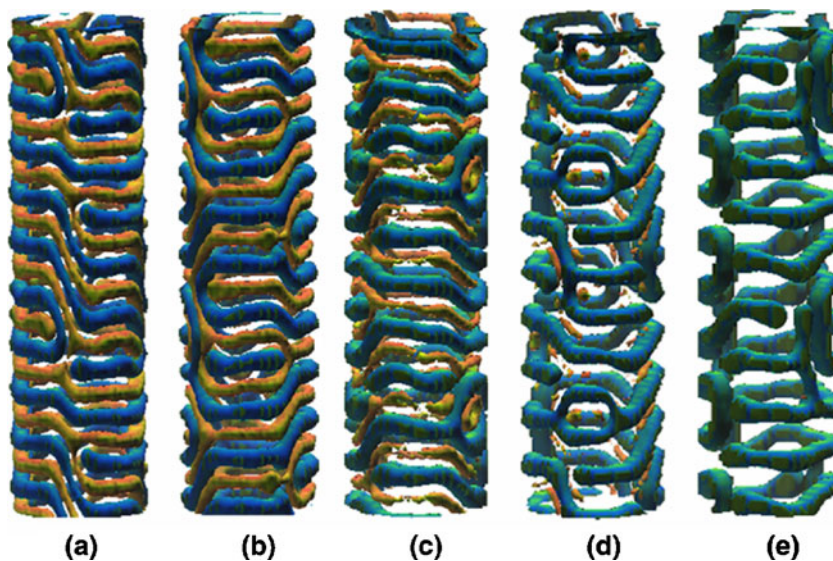
In order that the solvophobic block B can aggregate on the surface of the nanotube model, the last B bead in the polymer A_nB_{N-n} was selected to interact with the model surface. Thus the polymer can also be defined as $A_nB_{N-n-1}B'$,

where B' represents an attractive terminal B bead with the nanotube surface, and others (*i.e.*, S, A or B bead) repel the surface. For all simulations, the dimensionless parameters in MesoDyn program have been chosen as (see details in refs [25, 31]): the time step $\Delta\tau$=50 ns (dimensionless time step $\Delta\tau$=0.5), the noise scaling parameter Ω=100, the compressibility parameter $\kappa'_H = 25$, the grid parameter $d = ah^{-1} = 1.1543$, and the total simulation time is 50,000 steps (*i.e.*, 2.5 ms). The simulations were performed at 298 K. All the simulations were carried out using the MesoDyn module in the commercial software package Material Studio (version 4.1).

Results and discussion

Since the confinement of the polymers is soft, the nanotube surface is not necessarily cylindrical and can be developed into an outer fuzzy layer of the solvophobic block B. At

Fig. 3 Solvent Helixes displayed at various interaction parameter sets of. χ_{AS}/χ_{BS} (**a**) 0.82, (**b**) 0.65, (**c**) 0.47, (**d**) 0.29, (**e**) 0.12. Solvent-phase concentration field is as shown in Fig. 1
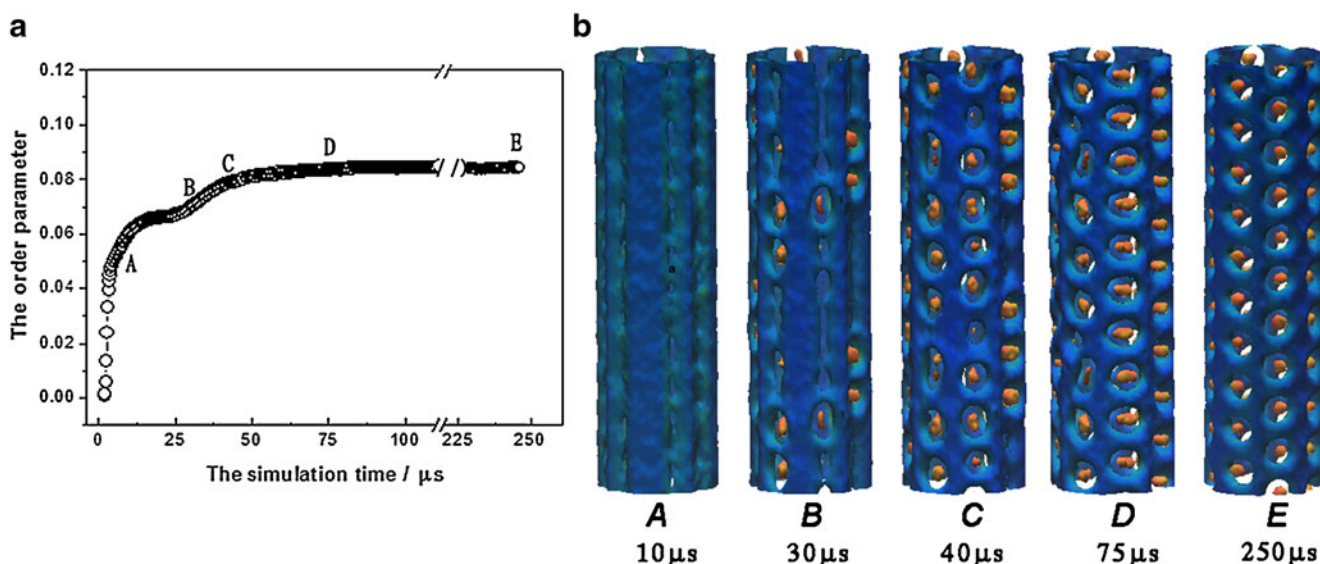
Fig. 4 Time evolution of the dimensionless order parameter: the curve refers to bead B. In (**b**), A to E are the morphologies corresponding to the parameter in (**a**). Solvent-phase concentration field is as shown in Fig. 1
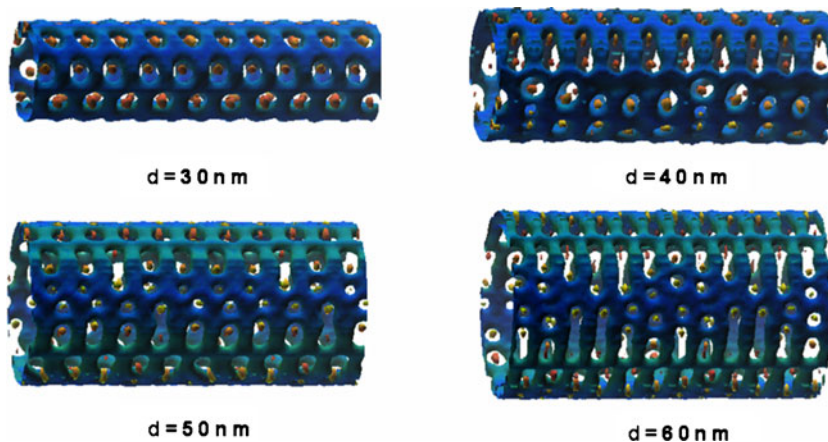
equilibrium, a mixture of 85 vol% of this particular polymer surfactant and hence 15 vol% of the solvent forms the nanotubes. The nanotube morphologies depending on the size ratio $f = n/N$ are shown in Fig. 1. On the surface, there exist numerous small valleys, ridges, and circles; and the systems structurally resemble much of the features in carbon nanotubes.

In the calculation, by observation the size ratio f can be used to control the structure and shape of the nanotubes (Fig. 1). In the case of $f=0.25$, the layers are characterized with pores, and the entire structure is a bicontinuous phase. The nanotube strikingly resembles a carbon nanotube with all the pores of a hexagonal pattern within the layer. When f is larger than 0.30, the hexagons are extended and a separated solvent phase with high density is clearly located in the center of the hexagons. As f increases to 0.5, there are two separated solvent phases segregating into two distinct helixes in the nanotube. There are no crossovers for the two helixes on the nanotube surface. At equilibrium, the nanotubes with hexagons ($f>0.25$) should

contain an appreciable amount of solvent distributed inhomogeneously over the solvophilic A and solvophobic B-rich layers. Thus, different patterns with different densities of the solvent phases are formed. When the ratio f is below 0.25, the solvophobic B block prefers sorption on the nanotube surface and aggregates in the solution, and is unable to form any patterned internal structure.

As shown in Fig. 2, with the increase of the polymer concentration when f is fixed at 0.25, the chains of solvophobic B block tend to aggregate, and the solvent sets apart the solvophobic phase. Different morphologies are formed, such as spherical micelles (Fig. 2a), worm-like micelles (Fig. 2b), and bicontinuous phase (Fig. 2c, d). As the polymer concentration increases up to certain level, ordered nanotube morphology looks like carbon nanotube is formed (Fig. 2e, f). It is interesting to note that additional high-density solvent phases are located in all hexagonal pores. That is, with the decrease of solvent concentration,

Fig. 5 Morphologies of the nanotubes at different diameters (**d**). Solvent-phase concentration field is as shown in Fig. 1

the solvent will be divided into a solvophobic B phase and a solvophilic A phase, respectively. In the solvophobic block B phase, the solvent has lower density. It is worth noting that the morphology is slightly changing when the concentration is more than 65 vol%.

Some previous works have demonstrated that the amphiphilic block copolymers can assemble into diverse microstructures with different Flory-Huggins interaction parameters [11]. As a check, the effects of different solvophilic interaction on the helical patterns of the solvent phase have been studied. With χ_{BS} fixed, the effect of χ_{AS} on the morphology of the polymer was assessed. Figure 3 presents the morphologies ($\chi_{AS}/\chi_{AB} = 0.47$) at different χ_{AS}/χ_{BS} from 0.82 to 0.12. The decrease in χ_{AS} means an increase in the solubility for block A. One of the helixes with high-density solvophilic phase disappears when χ_{AS} is one tenth of χ_{BS}. It is probably that the better solubility of block A makes the diffusion of the solvent easier in the micro-domain. Two distinct solvent helixes become one helix when χ_{AS} turns more solvophilic. When χ_{AS}/χ_{BS} is varying between 0.65 to 0.82, the two different helixes can be viewed as distinct channels in drug delivery or fabricating templates for example. The simulations reveal that the solvophobic block B can easily aggregate in the solvent due to the repulsion between the block B and solvent, and the block B mainly affects the morphology of the patterned nanotubes.

According to the discussion above, a system with parameters $\chi_{AB} \bullet N = 60$, $\chi_{AS}/\chi_{AB} = 0.47$, $\chi_{AS}/\chi_{BS} = 0.82$, and $\theta = 85$ vol% was selected to investigate the formation of the structure of the nanotube evolved with time. No micelle formation was observed when the system was still in non-equilibrium state initially ($t<0.01 ms$) (phases A and B in Fig. 4b). The order parameter increased rapidly and the solution was becoming homogeneous. After $0.04 ms$, the raw morphology of the nanotube was formed (phase C) with some defects. Finally at $0.25 ms$, a nanotube with patterns of hexagons like carbon nanotube fully came into being (phase E). The order parameter showed the change from the raw to the ordered nanotube (Fig. 4a). This process was time-consuming which took about $0.2 ms$. The morphologies of the nanotubes at different diameters ($f=0.25$) are also displayed in Fig. 5. Since the concentration and N of the polymer are constant, the number of pores can be determined from the radius. The physical and chemical properties of the nanotubes, which depend on the nanotube diameter, make them particularly attractive for future molecular nanotechnological applications.

Conclusions

In summary, we have reported a mesoscale long-time simulation based on MesoDyn to monitor nanotube self-assembly process of polymer surfactant in an aqueous bath. Nanotubes with hexagons formed by AB block copolymer, like carbon nanotube, were obtained at moderate ratio of amphiphilic and amphophobic solvent blocks. It is interesting to note that their morphological patterns are related to the polymer concentration, polymer-solvent interaction parameter and the diameter of the nanotubes. Since the mesoscale properties of polymer can be directly explored from simulation, we believe that the approach reported in this work will furnish important and useful information to experiments of amphiphilic polymer nanotubes.

References

1. Martin CR (1994) Nanomaterials: A membrane-based synthetic approach. Science 266:1961–1966
2. Schnur JM (1993) Lipid tubules-apardigm for molecularly engineered structures. Science 262:1669–1676
3. Rupert BL, He RR, Hochbaum A, Arnold J, Yang PD (2005) Synthesis of bifunctional polymer nanot uses from silicon nano-wire templates via atom transfer radical polymerization. J Am Chem Soc 127:16040–16041
4. Ghadiri M, Granja JR, Buehler LK (1994) Artificial transmembrane ion chanels from self-assembling peptide nanotubes. Nature 369:301–304
5. Qiu H, Wan M, Matthews B, Dai L (2001) Conducting polyaniline nanotubes by template-free polymerization. Macromolecules 34:675–677
6. Rodriguez AT, Chen M, Chen Z, Brinker CJ, Fan HY (2006) Nanoporous carbon nanotubes synthesized through confined hydrogen-bonding selfassembly. J Am Chem Soc 128:9276–9277
7. Mazur M, Tagowska M, Pałys B, Jackowska K (2003) Template synthesis of polyaniline and poly(2-methoxyaniline) nanotubes comparison of the formation mechanisms. Electrochem Commun 5:403–407
8. Bognitzki M, Hou H, Ishaque M, Frese T, Hellwig M, Schwarte C, Schaper A, Wendorff JH, Greiner A (2000) Polymer, Metal, and Hybrid Nano- and Mesotubes by Coating Degradable Polymer Template Fibers (TUFT Process). Adv Mater 12:637–640
9. Hou H, Jun Z, Reuning A, Schaper A, Wendorff JH, Greiner A (2002) Poly(p—xylylene) nanotubes by coating and removal of ultrathin polymer template fibers. Macromolecules 35:2429–2431
10. Giacomelli C, Schmidt V, Borsali R (2007) Figure 1Nanocontainers Formed by Self-Assembly of Poly(ethylene oxide)-b-poly(glycerol monomethacrylate)—Drug Conjugates. Macromolecules 40:2148–2157
11. Fermeglia M, Pricl S (2007) Multiscale modeling for polymer systems of industrial interest. Prog Org Coat 58:187–199
12. Lau KT, Gu C, Hui D (2006) A critical review on nanotube and nanotube/nanoclay related polymer composites materials. Composites Part B 37:425–436
13. Yang MJ, Koutsos V, Zaiser M (2005) Interactions between polymers and carbon nanotubes: A molecular dynamics study. J Phys Chem B 109:10009–10014

14. Feng J, Ruckenstein E (2006) Morphologies of AB diblock copolymer melts confined in nanocylindrical tubes. Macromolecules 39:4899–4906

15. Feng J, Ruckenstein E (2008) Self-assembling of hydrophobic-hydrophilic copolymers in hydrophobic nanocylindrical tubes: Formation of channels. J Chem Phys 128:074903(1–7)

16. Sevink GJA, Zvelindovsky AV, Fraaije JGEM, Huinink HP (2001) Morphology of symmetric block copolymer in a cylindrical pore. J Chem Phys 115:8226–8230

17. Feng J, Liu H, Hu Y (2007) Flow-induced morphologies of diblock copolymers in a nanotube studied by dissipative particle dynamics simulation. Fluid Phase Equilib 261:50–57

18. Feng J, Ruckenstein E (2006) Morphology transitions of AB diblock copolymer melts confined in nano cylindrical tubes. J Chem Phys 125:164911(1–6)

19. Wu Y, Cheng G, Katsov K, Sides SW, Wang J, Tang J, Fredrickson GH, Moskovits M, Stucky GD (2004) Composite mesostructures by nano-confinement. Nat Mater 3:816–822

20. Li W, Wickham RA, Garbary RA (2006) Phase diagram for a diblock copolymer met under cylindrical confinement. Macromolecules 39:806–811

21. Li W, Wickham RA (2006) Self-assembled morphologies of a diblock copolymer melt confined in a cylindrical nanopore. Macromolecules 39:8492–8498

22. Feng J, Ruckenstein E (2007) Self-assembling of ABC linear triblock copolymers in nanocylindricl tubes. J Chem Phys 126:124902 (1–8)

23. Fraaij JGEM, van Vlimmeren BAC, Maurlts NM, Postma M, Evers OA, Hoffmann C, Altevogt P, Goldbeck-Wood G (1997) The dynamic mean-field density functional method and its application to the mesoscopic dynamics of quenched block copolymer melts. J Chem Phys 106:4260–4269

24. Ludwigs S, Krausch G, Magerle R (2005) Phase behavior of ABC triblock terpolymers in thin films:Mesoseale simulations. Macromolecules 38:1859–1867

25. Fraaije JGEM, Sevink GJA (2003) Model for pattern formation in polymer surfactant nanodroplets. Macromolecules 36:7891–7893

26. Ma JW, Li X, Tang P, Yang YL (2007) Self-assembly of amphiphilic ABC star triblock copolymers and their blends with AB diblock copolymers in solution: Self-consistent field theory simulations. J Phys Chem B 111:1552–1558

27. Zhang LS, Lin JP, Lin SL (2007) Self-assembly behavior of amphiphilic block copolymer/nanoparticle mixture in dilute solution studied by self-consistent-field theory/density functional theory. Macromolecules 40:5582–5592

28. Wang R, Tang P, Qiu F, Yang YL (2005) Aggregate morphologies of amphiphilic ABC triblock copolymer in dilute solution using self-consistent field. Theor J Phys Chem B 109:17120–17127

29. Altevogt P, Evers OA, Fraaije JGEM, Maurits NM, van Vlimmeren BAC (1999) The MesoDyn project: Software for mesoscale chemical engineering. J Mol Struct Theochem 463:139–143

30. Fraaij JGEM, van Vlimmeren BAC, Maurlts NM, Postma M (1997) Application of free energy expansions to mesoscopic dynamics of copolymer melts using a Gaussian chain molecular model. J Chem Phys 106:6730–6743

31. Guo SL, Hou TJ, Xu XJ (2002) Simulation of the phase behavior of the $(EO)_{13}(PO)_{30}(EO)_{13}$(Pluronic L64)/Water/p-Xylene system using mesodyn. J Phys Chem B 106:11397–11403

32. Maurlts NM, van Vlimmeren BAC, Fraaij JGEM (1997) Mesoscopic phase separation dynamics of compressible copolymer melts. Phys Rev 56:816–825

33. Lam YM, Goldbeck-Wood G (2003) Mesoscale simulation of block copolymers in aqueous solution: Parameterisation, micelle growth kinetics and the effect of temperature and concentration morphology. Polymer 44(12):3593–3605

34. Maurits NM, Fraaije JGEM (1997) Application of free energy expansions to mesoscopic dynamics of copolymer melts using a Gaussian chain molecular model. J Chem Phys 106:6730–6743

35. Li YY, Hou TJ, Guo SL, Xu XJ (2000) The Mesodyn simulation of pluronic water mixtures using the 'equivalent chain' method. Phys Chem Chem Phys 2:2749–2753

36. Sevink GJA, Fraaije JGEM (2002) Structure of aqueous pluronics films: Dynamics of surface directed mesophase formation. Macromolecules 35:1848–1859

37. Zhang XQ, Yuan SL, Wu J (2006) Mesoscopic simulation on phase behavior of ternary copolymeric solution in the absence and presence of shear. Macromolecules 39:6631–6642

38. Yuan SL, Zhang XQ, Chen GY (2009) Effects of shear and charge on the microphase formation of P123 polymer in the SBA-15 synthesis investigated by mesoscale simulations. Langmuir 25:2034–2045

39. Li YM, Xu GY, Chen AM, Yuan SL (2005) Aggregation between xanthan and nonyphenyloxypropyl β-hydroxyltrimethylammonium bromide in squeous solution: MesoDyn simulation and binding isotherm measurement. J Phys Chem B 109:22290–22295

40. van Vlimmeren BAC, Maurits NM, Zvelindovsky AV, Sevink GJA, Fraaije JGEM (1999) Simulation of 3D mesoscale structure formation in concentrated aqueous solution of the triblock polymer surfactants (ethylene oxide)$_{13}$-(propylene oxide)$_{30}$(ethylene oxide)$_{13}$ and (propylene oxide)$_{19}$—(ethylene oxide)$_{33}$(propylene oxide)$_{19}$. Macromolecules 32:646–656

41. Tyler CA, Qin J, Bates FS, Morse DC (2007) SCFT study of nonfrustrated ABC triblock copolymer melts. Macromolecules 40:4654–4668

42. Yu YS, Zhang LF, Eisenberg A (1998) Morphogenic effect of solvent on crew-cut aggregates of apmphiphilic diblock copolymers. Macromolecules 31:1144–1154

43. Hamley IW, Castelletto V (2001) Melt phase behavior of poly (oxyethylene)-poly(oxypropylene) diblock copolymers. Macromolecules 34:4079–4081

44. Eliassi A, Modarress H, Mansoori GA (1999) Measurement of activity of water in aqueous poly(ethylene glycol) solutions (Effect of excess volume on the Flory-Huggins chi-parameter). J Chem Eng Data 44:52–55